The Structure of Liquid Silver-Copper Alloys*

W. E. Lukens

Materials Department, Naval Ship Research and Development Center
Annapolis, Maryland 21402

and C. N. J. Wagner

Materials Department, School of Engineering and Applied Science
University of California, Los Angeles, California 90024

(Z. Naturforsch. **30 a**, 242–249 [1975]; received November 22, 1974)

Mo-Kα X-rays have been used as a radiation probe to evaluate the interference functions $I(K)$ (also called structure factors) of liquid Ag, Cu and Ag-Cu alloys with 16.5, 28, 37, 50, 57, 71 and 85 at.% Cu at temperatures about 50 °C above the liquidus. Employing the transmission technique, $I(K)$ has been determined in the range of $K = 4\pi \sin\theta/\lambda$ between 0.8 and 12.5 Å^{-1}. The partial interference functions $I_{ij}(K)$ have been calculated, and it was found that the assumption of concentration independence of $I_{ij}(K)$ yielded reduced partial distribution functions $G_{ij}(r)$, the weighted sum of which were in excellent agreement with $G(r)$, the Fourier transform of $F(K) = K[I(K) - 1]$. The position r_1 of the first peak in $G(r)$ and the coordination number η show a positive deviation from a straight line when plotted as a function of concentration.

I. Introduction

The structure of a binary liquid alloy is completely characterized by the three atomic distribution functions $\varrho_{11}(r)$, $\varrho_{12}(r)$, and $\varrho_{22}(r)$, which can, in principle, be determined from diffraction experiments [1–3]. In general, $\varrho_{ij}(r)$ represents the number of j-type atoms per unit volume at the distance r from an i-type atom.

Diffraction experiments, using X-rays, electrons or neutrons as the radiation probe, yield only the total interference function $I(K)$ (also called structure factor of the liquid). It can be shown [4] that

$$I(K) = \sum_i \sum_j W_{ij}(K)\, I_{ij}(K) \qquad (1)$$

where

$$W_{ij}(K) = c_i c_j f_i f_j / \langle f \rangle^2 . \qquad (2)$$

c_i and f_i are the atomic concentration and scattering factor of atoms of type i, respectively, $\langle f \rangle = \sum_i c_i f_i$ is the average scattering factor of the alloy, $K = 4\pi \sin\theta/\lambda$, and

$$I_{ij}(K) = 1 + \int_0^\infty 4\pi r^2 \varrho_0 [g_{ij}(r) - 1] \frac{\sin K r}{K r}\, \mathrm{d}r , \qquad (3)$$

is the partial interference function. It is the Fourier transform of the pair distribution function $g_{ij}(r) = \varrho_{ij}(r)/(c_j \varrho_0)$, where ϱ_0 is the average atomic density of the alloy. The function $g_{ij}(r)$ is obtained from $G_{ij}(r)$ which is the Fourier transform of $K[I_{ij}(K) - 1]$, i. e.,

$$G_{ij}(r) = 4\pi r \varrho_0 [g_{ij}(r) - 1] = \frac{2}{\pi} \int_0^\infty K[I_{ij}(K) - 1] \sin K r\, \mathrm{d}K . \qquad (4)$$

Commonly, the Fourier transform of the total interference function $I(K)$ is calculated and called the total distribution function $g(r)$, which is related to the reduced atomic distribution function $G(r)$, i. e.,

$$G(r) = 4\pi r \varrho_0 [g(r) - 1] = \frac{2}{\pi} \int_0^\infty K[I(K) - 1] \sin K r\, \mathrm{d}K . \qquad (5)$$

Applying the convolution theorem of Fourier transforms, one obtains immediately the relationships [4, 5]:

$$F(K) = K[I(K) - 1] = \sum_i \sum_j W_{ij}(K)\, F_{ij}(K) \qquad (6)$$

and

$$G(r) = 4\pi r \varrho_0 [g(r) - 1] = \sum_i \sum_j w_{ij}(r) * G_{ij}(r) \qquad (7)$$

where

$$F_{ij}(K) = K[I_{ij}(K) - 1].$$

The star (*) represents the convolution product. Only when $W_{ij}(K)$ is independent of K can we write

$$G(r) = 4\pi r \varrho_0 [g(r) - 1] = \sum_i \sum_j w_{ij}\, G_{ij}(r) , \qquad (8)$$

* Research supported by the U.S. Atomic Energy Commission.

Reprint requests to Prof. C. N. J. Wagner, Materials Department, School of Engineering and Applied Science, University of California, *Los Angeles, California 90024*, USA.

because $w_{ij}(r) = W_{ij}\,\delta(r)$, which represents the Warren-Krutter-Morningstar (WKM) approximation [6].

The purpose of this investigation was to measure the total interference functions of liquid Ag-Cu alloys over a wide range of K, using the transmission technique, and to determine the partial interference functions $I_{ij}(K)$ with the assumption that they are independent of the concentration of the alloys.

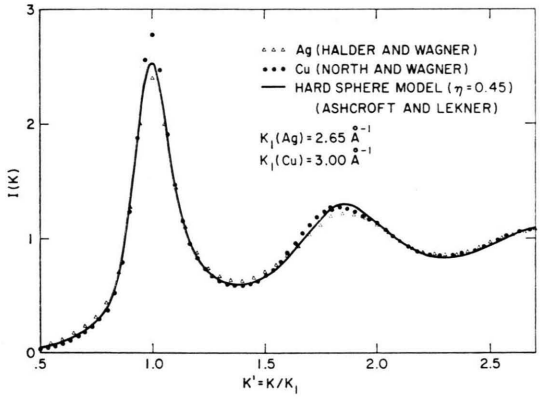

Fig. 1. Interference functions of Ag (△) and Cu (●) measured with the reflection technique by Halder and Wagner [7] and North and Wagner [8]. Solid curve represents hardsphere model of Ashcroft and Lekner [9].

As shown in Fig. 1, the structures of both liquid Ag and Cu, which were determined previously [7, 8] can be described by the hard-sphere model $I(K)$ of Ashcroft and Lekner [9] with a packing density $\eta = 0.45$. In addition, the coordination numbers of these liquid metals lie between 11 and 12 indicating that they retain a close packing in the liquid state. It is, therefore, assumed that the local atomic arrangements are similar in liquid Ag-Cu alloys with different concentrations. However, Ag and Cu atoms have different atomic sizes, which are responsible for the difference in positions of the minima and maxima in the $g(r)$ curves, and consequently in $I(K)$, as observed experimentally [see Fig. 1, where $K_1(\mathrm{Ag}) = 2.65$ Å^{-1} and $K_1(\mathrm{Cu}) = 3.00$ Å^{-1}]. Therefore, the positions K_n of the mixture of $I(K)$ should move continuously from the values observed for pure Ag to those of pure Cu. Since this shift is already considerable for the first peak, it should be possible to deduce the three partial functions by least square analysis of more than three total interference functions of the alloys with different concentrations.

II. Experimental Technique

A) Sample Preparation

Alloys of Ag and Cu with 16.5, 28, 37, 50, 57, 71 and 85 at.% Cu were prepared in graphite sample holders, suitable for the X-ray measurements, in the X-ray high-temperature furnace. Foils of Ag and Cu were rolled to thicknesses ranging from 5 μm to 25 μm. Alloys of the desired composition were made by sandwiching together foils of Cu and Ag of appropriate thicknesses. The compositions were determined from the weights of the elemental foils. The total thickness of each alloy foil was about 50 μm, reasonably close to the $1/e$ thickness (25 μm for Cu, and 50 μm for Ag using Mo Kα radiation) for maximizing the X-ray intensities in the transmission method [4].

In order to assure complete solubility of the pure elements in each other in the liquid state, both Ag and Cu were cleaned in appropriate acid etches (Cu first in 50% HNO_3 – 50% H_2O, then in 50% HCl – 50% H_2O; Ag in 50% HNO_3 – 50% H_2O only). After etching, the foils were rinsed in triply distilled water, dried on ashless filter paper in an argon atmosphere, immediately placed in the sample holder, and transferred to the high-temperature furnace. After evacuation of the camera and subsequent flooding with a 80% He – 20% H mixture, the furnace was turned on, and the temperature raised to approximately 50 °C above the melting point at a rate of 300 °C per minute.

B) X-Ray Technique

All scattering data were obtained with the transmission technique, which has been described by North and Wagner [10] and subsequently modified by Lukens and Wagner [11]. X-rays from a line source with a Mo target impinged on a flat graphite monochromator, which produced a very narrow beam of high intensity. In order to simplify absorption corrections, and to reach the highest possible angle for a given sample width (5 mm), the liquid sample was rotated at half angular speed of that of the detector.

The sample holder consisted of two pyrolitic graphite sheets (each 0.13 mm thick) sandwiched between two graphite formers with a vertical window, 5 mm wide and 16 mm high.

The experiments were run in an 80% He and 20% H atmosphere at temperatures ranging from 20 °C to 70 °C above the melting point of each alloy. The exact temperatures are indicated in Figure 2.

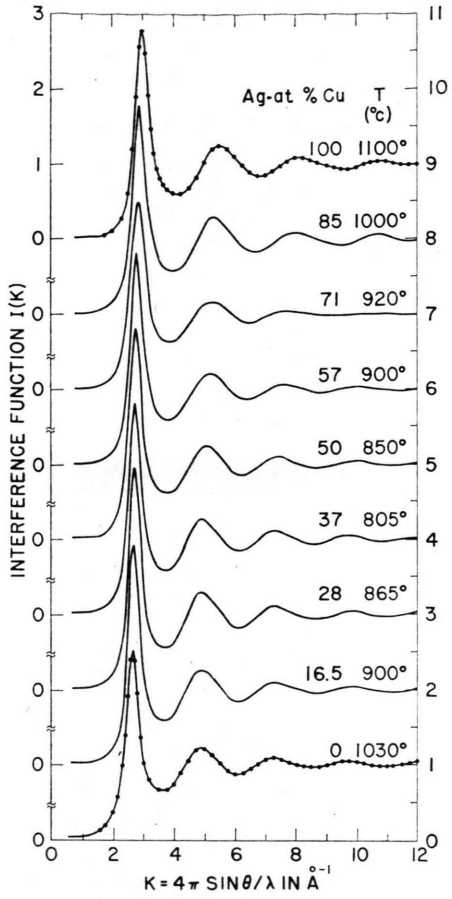

Fig. 2. Total interference functions of liquid Ag, Cu and Ag-Cu alloys. Solid dots represent data of Halder and Wagner [7] for pure Ag, and North and Wagner [8] for pure Cu.

C) Data Reduction and Analysis

The transmission technique enabled us to measure the scattered X-ray intensities in the range of K between 0.8 and 12.5 $Å^{-1}$. The sample holder scattering $I_s(2\theta)$ was determined in a separate experiment and, after correction for absorption in the alloy sample, subtracted from the total scattering $I_{tot}(2\theta)$, thus yielding the sample intensity $I_f(2\theta)$. The value of μt of the sample was obtained by measuring the attenuation of the primary beam whose intensity was greatly reduced by a 25 μm Ta foil, and its $\lambda/2$ component completely removed by lowering the voltage to 30 kV.

To obtain the coherent intensity per atom, $I_a(K)$, the sample intensity $I_f(2\theta)$ was corrected for polarization and absorption in the sample, and, after conversion from the 2θ scale to $K = 4\pi \sin\theta/\lambda$, normalized to absolute units, i. e., the scattered intensity expressed in electron units [4]. The average of values of the normalization procedures, i. e., the high angle method [4] and the radial distribution function method [4], was used in this investigation.

III. Experimental Results

A) Interference Function (Structure Factor) of Liquid Ag-Cu Alloys

The total interference functions $I(K)$ of Ag, Cu, and the Ag-Cu alloys are shown in Figure 2. The temperatures of measurements are indicated in the diagrams. The dots on the pure Ag, and Cu curves represent the data of Halder and Wagner [7], and North and Wagner [8], respectively, measured previously on a theta-theta diffractometer in reflection. As is readily apparent, the agreement between the transmission and reflection data is excellent.

The values K_n of the positions of the first three maxima of $I(K)$, i. e., K_1, K_2, and K_3 are given in Figure 3. All K_n vary continously from pure Ag

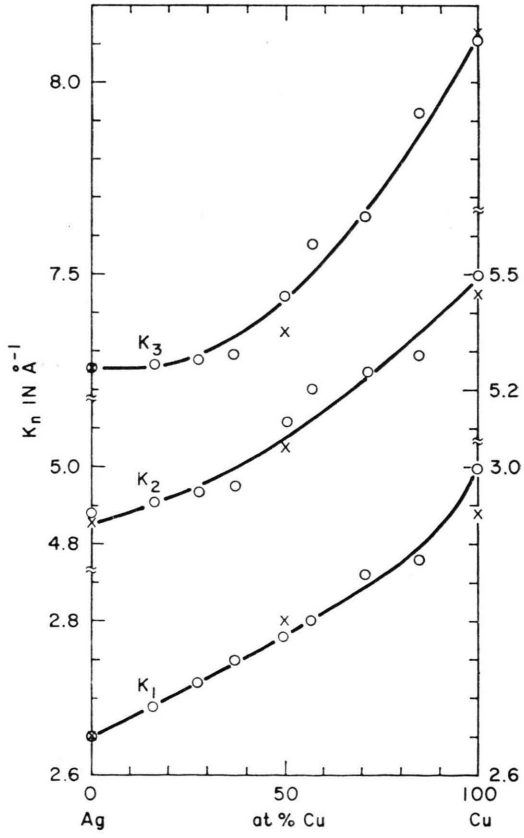

Fig. 3. Positions K_n of the first three peak maxima of $I(K)$ for Ag-Cu alloys. (○) K_n of the $I(K)$; (×) K_n of the $I_{ij}(K)$.

to the pure Cu value; initially more slowly with increasing Cu concentration because of the larger scattering power of Ag in the factor $W_{ij}(K)$ of Equation (1).

Because of the smooth variation of the positions K_n of $I(K)$ as a function of concentration, and the fact that both $I(K)$ of Ag and Cu could be matched with the hard-sphere model, it was felt that the assumption of concentration independence of the partial interference functions $I_{ij}(K)$ might be quite reasonable. Therefore, the three partial functions $I_{AgAg}(K)$, $I_{AgCu}(K)$, and $I_{CuCu}(K)$ have been determined by a least squares analysis using the $I(K)$ of the alloys only. Figure 4 shows the partial functions

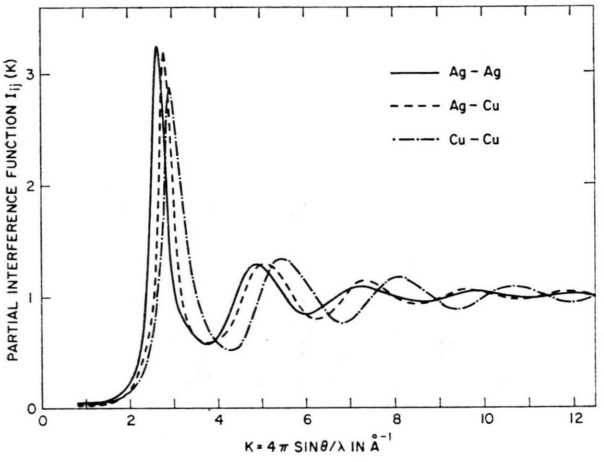

Fig. 4. Partial interference functions $I_{AgAg}(K)$, $I_{CuCu}(K)$ and $I_{AgCu}(K)$ evaluated from the total $I(K)$ of the Ag-Cu alloys.

$I_{ij}(K)$. On including the $I(K)$ of the pure elements in the least squares analysis, $I_{ij}(K)$ were obtained which were almost identical to those shown in Fig. 4, as far as the positions K_n of the maxima were concerned. However, there was a slight increase in height of the first peak in $I_{AgCu}(K)$ obtained from the alloys' and elements' data. The values of K_n of the maxima of the partial $I_{ij}(K)$ function, deduced from the alloy data only, are shown in Figure 3.

B) Atomic and Radial Distribution Function

The Fourier transforms of the partial interference functions $I_{ij}(K)$, i. e., the reduced partial atomic distribution functions $G_{ij}(r)$ are shown in Figure 5. The Fourier transforms of the total interference functions $I(K)$, i. e., the reduced total atomic distribution functions $G(r)$ are shown in Figure 6.

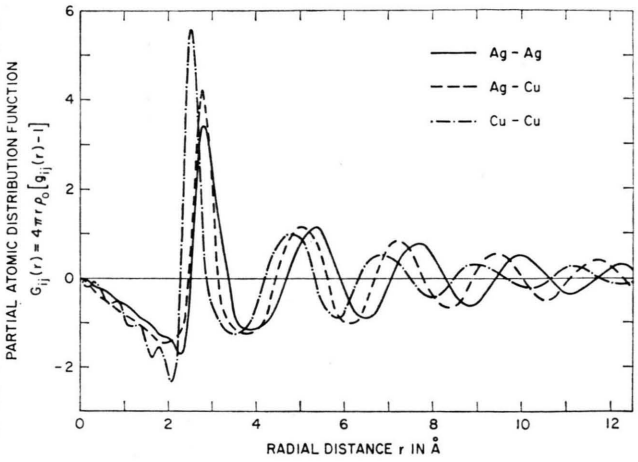

Fig. 5. Reduced total atomic distribution functions $G(r)$ which represent the Fourier transforms of $K[I(K) - 1]$.

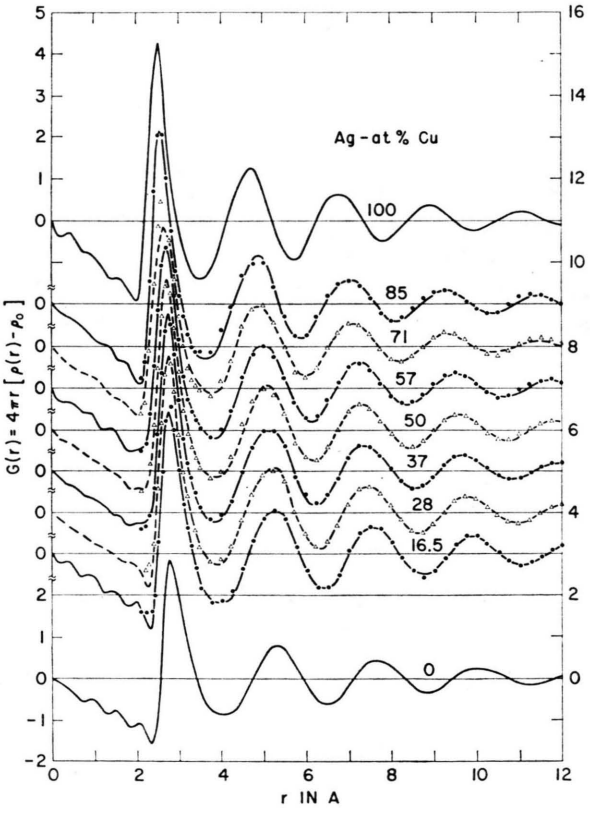

Fig. 6. Reduced total atomic distribution functions $G(r)$ which are the Fourier transforms of $K[I(K) - 1]$. The triangles and dots represent the weighted sum of the partial atomic distribution functions, i. e., $\sum_i \sum_j W_{ij} G_{ij}(r)$.

The positions r_1 and r_2 of the first two peaks of $G_{ij}(r)$ and $G(r)$ are given in Figure 7.

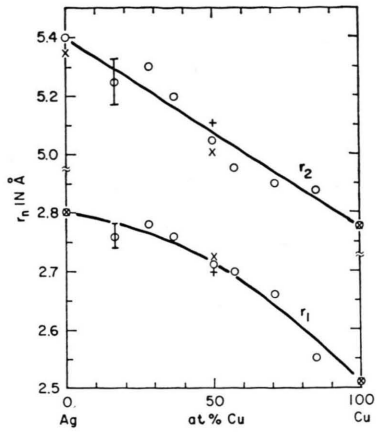

Fig. 7. Positions r_n of the first two peak maxima of $G_{ij}(r)$ and $G(r)$ in Ag-Cu alloys. (○) r_n of $G(r)$; (×) r_n of $G_{ij}(r)$, deduced from the alloy data only; (+) r_n of $G_{\mathrm{AgCu}}(r)$, deduced from alloy and pure element data.

The radial distribution functions (RDF)

$$4\pi r^2 \varrho(r) = 4\pi r^2 \varrho_0 + r\,G(r)$$

of the alloys are illustrated in Figure 8. The area

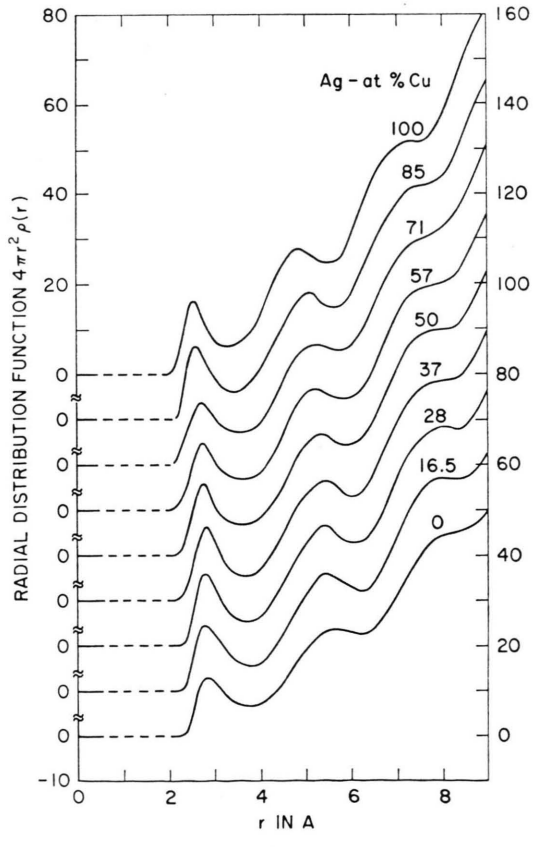

Fig. 8. Radial distribution function $4\pi r^2 \varrho(r)$ of Ag-Cu alloys.

under the first peak of each RDF, which represents the coordination number η, was determined as

$$\eta = \int_0^{r_0} 4\pi r^2 \varrho(r)\,\mathrm{d}r\,, \qquad (9)$$

where r_0 is the position of the minimum after the first peak. The coordination numbers η are shown in Figure 9.

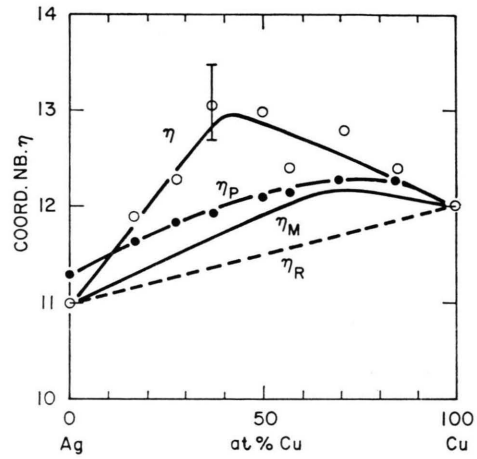

Fig. 9. Coordination number η of Ag-Cu alloys. η_R represents the variation of η in a random alloy as a function of concentration [Equation (11)]. η_M are the values evaluated with Eq. (10) (macrosegregation) and η_P are the values obtained from the partial η_{ij} with Equation (12).

It is also possible to calculate the number n of electrons in the first coordination shell from the coordination η, i. e.,

$$n = \eta \langle Z \rangle$$

where $\langle Z \rangle = \sum_i c_i Z_i$, Z_i being the atomic number of element i. The values of n are plotted in Figure 10.

IV. Discussion

A) Interference Function

It is apparent from the total interference functions $I(K)$ (Fig. 2) that the structure of the Ag-Cu alloys does not show any unusual features, such as the splitting of the first peak which is observed in Cu-Sn alloys [8], or a premaximum below the first peak found in Cu-Mg alloys [11]. In addition, the positions K_n of the peak maxima vary smoothly from the values observed in pure Ag to those in pure Cu as shown in Figure 3.

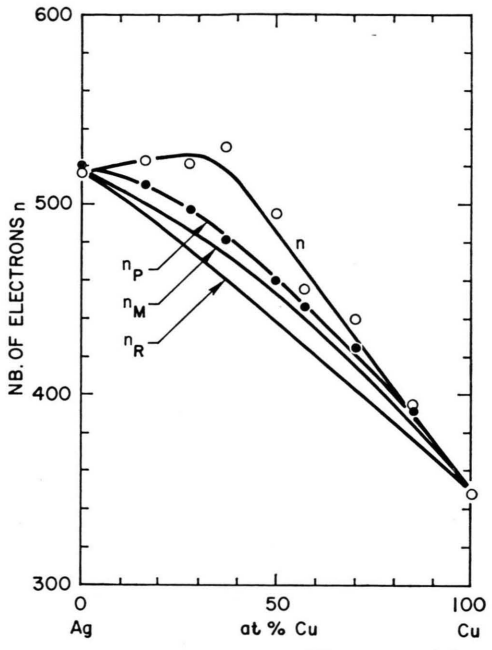

Fig. 10. Number of electrons $n=\langle Z\rangle$, where $\langle Z\rangle$ is the average number of electrons per atom in the alloy plotted as a function of Cu concentration. n_R, n_M and n_P were calculated from η_R, η_M and η_P.

The absence of the splitting of the first peak in $I(K)$ indicates that the partial function $I_{AgCu}(K)$ must fall in between the functions $I_{AgAg}(K)$ and $I_{CuCu}(K)$, which is indeed shown in Figure 4. A similar behavior was found in Ag-Sn alloys [7], and can be explained with the hard-sphere model of liquid alloys [12, 13]. However, a splitting of the first peak of $I(K)$ of the Cu – 55 at.% Sn alloy was observed in spite of the fact that the partial function $I_{CuSn}(K)$ falls in between those of $I_{CuCu}(K)$ and $I_{SnSn}(K)$. The reason for the splitting is found in the large difference $\Delta K = K_1(\mathrm{Cu}) - K_1(\mathrm{Sn}) = 0.75$ Å^{-1} in position of the first peaks for Cu and Sn, and the effect of Sn in the weighting factor $W_{ij}(K)$ [Eq. (2)] in the total $I(K)$ [Equation (1)]. Although the weight of Ag in W_{ij} is similar to that of Sn, the difference $\Delta K = K_1(\mathrm{Cu}) - K_1(\mathrm{Ag}) = 0.35$ is only half of that observed in Cu-Sn, and too small to produce a splitting of the first peak. It should be noted that $\Delta K = K_1(\mathrm{Ag}) - K_1(\mathrm{Sn}) = 0.40$ is similar to ΔK(Cu-Ag), and no splitting has been observed in Ag-Sn alloys, as mentioned above.

In contrast, liquid Au-Sn alloys were the first system where the double peak in the scattering pattern has been found [14]. The double peak or splitting of the first peak in $I(K)$ is particularly noticeable in the alloy with 67 at.% Sn [2]. Since the separation of the first peak maxima of Au and Sn is the same as that of Ag and Sn, because the interference functions of Ag and Au are practically identical [15], the splitting must be due to the fact that the partial function $I_{AuSn}(K)$ does not follow the pattern exhibited by CuSn, AgSn or AgCu. Indeed, the experimental function $I_{AuSn}(K)$ can be reproduced rather well by Fourier transformation of an atomic distribution similar to an ordered AuSn alloy with NiAs structure as shown by Kaplow et al. [2]. Its first peak is even at higher value, K_1 ($= 2.94$ Å^{-1}) than that of Au ($K_1 = 2.67$ Å^{-1}).

The partial interference functions $I_{AgAg}(K)$ and $I_{CuCu}(K)$ are practically identical with those observed in pure Ag, and pure Cu, respectively. However, in the case of Cu, the position K_1 of the first peak in the partial function is slightly smaller ($K_1 = 2.94$ Å^{-1}) than that observed in the pure liquid copper. A similar discrepancy has been observed in the partial function $I_{CuCu}(K)$ in Cu-Sn alloys [8].

B) Atomic Distribution Function

The Fourier transforms of the partial interference functions, i. e., the reduced partial atomic distribution functions $G_{ij}(r)$ can be described fairly well with a hard-sphere model of liquid alloys [12, 13]. The positions of the peak maxima of the reduced functions $G_{AgAg}(r)$ and $G_{CuCu}(r)$ are practically identical with those observed in the pure liquids. Only the position of the first peak of $G_{AgCu}(r)$ shows a positive deviation from a linear interpolation between the values of pure Ag and Cu.

In order to test Eq. (8) which represents the (WKM) approximation [4], the total reduced distribution function, calculated from the total interference function [Eq. (5)] and represented as solid or dashed curves in Fig. 6, were compared with $G(r)$, evaluated with Eq. (8) and represented as dots or triangles in Figure 6. It is obvious that the agreement between the $G(r)$ curves is excellent, indicating that the partial functions $G_{ij}(r)$ are representative of the distributions of atoms about the Ag or Cu atoms over short distances of r ($r < 20$ Å). Similar observations have been made in Cu-Sn and Ag-Sn alloys [7, 8]. However, as soon as strong compound formation or ordering (as evidenced by a premaximum) occurs in the binary alloy system, the partial functions cannot be assumed to be independent of

concentration. Such behavior has been observed in liquid Mg-base alloys [11, 16, 17] and Li-base alloys [18].

Because the solid, binary phase diagram of Ag and Cu is of the eutectic type, a preference for like neighbors might even persist in the liquid. That such a tendency exists, can be deduced from the variation of the coordination number η as a function of concentration. As shown by Steeb and Hezel [19], assuming that the number of AB pairs is small compared to the number of AA or BB pairs (macrosegregation), we can write

$$\eta_M = \frac{c_1 Z_1^2 \eta_1 + c_2 Z_2^2 \eta_2}{\langle Z \rangle^2} \qquad (10)$$

where Z_1 and Z_2 are the number of electrons in element 1 and 2, respectively, and η_1 and η_2 are the coordination numbers in the liquids of elements 1 and 2, respectively. If the atoms were randomly distributed in the liquid alloy then:

$$\eta_R = \langle \eta \rangle = c_1 \eta_1 + c_2 \eta_2 , \qquad (11)$$

i. e., η_R falls on a straight line when plotted as a function of concentration c_2. The values of η_M and η_R are plotted as a function of concentration of the Cu atoms in Figure 9. Since the experimental values of η, also represented as open circles in Fig. 9, show an even larger positive deviation from the random behavior than calculated on the assumption of macrosegregation in the liquid, it must be concluded that the arrangement of the AB pairs does play a role in average structure of the liquid.

The coordination number η_{ij} of the partial functions have also been calculated, and the values 11.3, 12.7, and 12.0 were obtained for the AgAg, AgCu and CuCu pairs, respectively. The value of 12.7 for η_{AgCu} is larger than either η_{AgAg} and η_{CuCu}, which are quite close to the values observed in the pure liquids, and might be responsible for the deviation of η from the random distribution. It is easily seen that the coordination number η_P can be calculated from η_{ij} by the relation:

$$\eta_P = \sum_i \sum_j w_{ij} \eta_{ij} . \qquad (12)$$

The values of η_P are also plotted in Fig. 9 as filled circles, and it is obvious from the curve that the agreement between η and η_P is relatively poor. However, the poor agreement does not arise from a breakdown of Eq. (8) which assumes that $W_{ij}(K)$ is independent of K. In the case of Ag-Cu alloys, the K-dependence of W_{ij} is reasonably small [11] so that any convolution broadening [Eq. (7)] of the first peak in $G(r)$ can be neglected. Even though the agreement between η and η_P is relatively poor, both curves indicate the same trend which is a strong positive deviation from a linear, or random behavior. The curves of Fig. 10 reinforce those of Fig. 9 in their indication of a positive deviation from random behavior in the Ag-Cu alloy system.

V. Summary and Conclusions

The scattering patterns of the Ag-Cu alloys can be interpreted as the weighted sum of $I_{ij}(K)$, derived from $I(K)$ of the alloys. This can be concluded from the fact that the Fourier transforms of $I_{ij}(K)$ yield $G_{ij}(r)$, which in turn reproduce $G(r)$, the transforms of $F(K) = K[I(K) - 1]$, of the alloys.

The position r_1 of the first peak in $G(r)$ and the coordination number η show a positive deviation from a straight line when plotted as a function of concentration. This behavior indicates that a tendency towards segregation might persist even in the liquid. In addition, since the experimental values of η show an even larger positive deviation from the random behavior than calculated on the assumption of macrosegregation in the liquid, it must be concluded that the arrangement of the AB pairs does play a role in average structure of the liquid.

[1] D. T. Keating, J. Appl. Phys. **34**, 923 [1963].
[2] R. Kaplow, S. L. Strong, and B. L. Averbach, Local Atomic Arrangement Studied by X-Ray Diffraction, J. B. Cohen and J. E. Hilliard (eds.), Gordon and Breach, New York 1966, p. 159.
[3] C. N. J. Wagner and N. C. Halder, Adv. Phys. **16**, 62 [1967].
[4] C. N. J. Wagner, Liquid Metals, Chemistry and Physics, S. Z. Beer (ed.), Moral Dekker, New York 1972, p. 257.
[5] C. J. Pings and J. Waser, J. Chem. Phys. **48**, 3016 [1968].
[6] B. E. Warren, X-Ray Diffraction, Addison-Wesley, Reading, Massachusetts 1969.
[7] N. C. Halder and C. N. J. Wagner, J. Chem. Phys. **47**, 4385 [1967].
[8] D. M. North and C. N. J. Wagner, Physics and Chemistry of Liquids **2**, 87 [1970].
[9] N. W. Ashcroft and J. Lekner, J. Phys. Rev. **145**, 83 [1966].
[10] D. M. North and C. N. J. Wagner, J. Appl. Cryst. **2**, 149 [1969].
[11] W. E. Lukens and C. N. J. Wagner, Z. Naturforsch. **28 a**, 297 [1973].

[12] N. W. Ashcroft and D. C. Lengreth, Phys. Rev. **156**, 685 [1967].
[13] J. E. Enderby and D. M. North, Phys. Chem. Liquids **1**, 1 [1968].
[14] H. Hendus, Z. Naturforsch. **2a**, 505 [1947].
[15] O. Pfannenschmid, Z. Naturforsch. **15a**, 603 [1960].
[16] S. Steeb and R. Hezel, Z. Metallkde **57**, 374 [1966].
[17] A. Boos, S. Steeb, and D. Godel, Z. Naturforsch. **27a**, 271 [1973].
[18] K. Goebbels and H. Ruppersberg, Prop. Liquid Metals, S. Takeuchi (ed.), Taylor and Francis, London 1973.
[19] S. Steeb and R. Hezel, Z. Phys. **191**, 398 [1966].